



## REVIEW

# From Macroscopic Measurements to Microscopic Mechanisms of Protein Aggregation

Samuel I. A. Cohen<sup>1,2</sup>, Michele Vendruscolo<sup>1</sup>,  
Christopher M. Dobson<sup>1</sup> and Tuomas P. J. Knowles<sup>1\*</sup>

<sup>1</sup>Department of Chemistry, University of Cambridge, Lensfield Road, Cambridge CB2 1EW, UK

<sup>2</sup>School of Engineering and Applied Sciences, Harvard University, 29 Oxford Street, Cambridge, MA 02138, USA

Received 22 November 2011;  
received in revised form  
21 February 2012;  
accepted 22 February 2012  
Available online  
8 March 2012

Edited by S. Radford

**Keywords:**

amyloid;  
kinetics;  
mechanism;  
aggregation;  
nucleation

The ability to relate bulk experimental measurements of amyloid formation to the microscopic assembly processes that underlie protein aggregation is critical in order to achieve a quantitative understanding of this complex phenomenon. In this review, we focus on the insights from classical and modern theories of linear growth phenomena and discuss how theory allows the roles of growth and nucleation processes to be defined through the analysis of experimental *in vitro* time courses of amyloid formation. Moreover, we discuss the specific signatures in the time course of the reactions that correspond to the actions of primary and secondary nucleation processes, and outline strategies for identifying and characterising the nature of the dominant process responsible in each case for the generation of new aggregates. We highlight the power of a global analysis of experimental time courses acquired under different conditions, and discuss how such an analysis allows a rigorous connection to be established between the macroscopic measurements and the rates of the individual microscopic processes that underlie the phenomenon of amyloid formation.

© 2012 Elsevier Ltd. All rights reserved.

## Introduction

The aggregation of protein molecules into filaments is a common form of biological homomolecular self-assembly. The resulting structures are involved in both functional and aberrant phenomena in nature, with examples ranging from the formation of functional actin filaments<sup>1–5</sup> to the pathological aggregation of hemoglobin S in sickle cell anemia.<sup>6–9</sup> There has been recently renewed interest in this phenomenon as it has become clear that many different peptide and protein molecules are able to self-assemble into amyloid fibrils, aggregates that share a common cross- $\beta$  sheet structure and that are associated with a range of increasingly prevalent clinical disorders,<sup>10–23</sup> including Alzheimer's and Parkinson's diseases.

A critical challenge in the study of protein aggregation is to relate the commonly available bulk experimental measurements to the microscopic steps in the mechanism of aggregation. Historically, as indeed for many other chemical reactions, major advances in the understanding of protein aggregation processes have been made through the study of rate laws governing the assembly pathway. Rate laws are the workhorses of chemical kinetics, but for complex assembly pathways, closed form expressions for the reaction rate are in general challenging to derive since the system consists of a very large number of molecular species with different polymerisation numbers and that can inter-convert through a multitude of processes. A major advance in this area came through the work of Oosawa who showed in the 1960s that the polymerisation of actin could be described by homogeneous (i.e., primary) nucleation of aggregates coupled to growth through monomer addition.<sup>1,2,24</sup> Oosawa derived an

\*Corresponding author. E-mail address: [tpjk2@cam.ac.uk](mailto:tpjk2@cam.ac.uk).

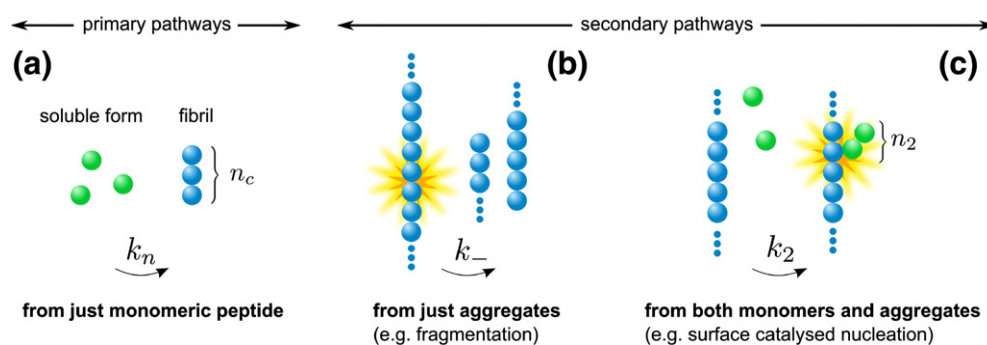


**Fig. 1.** The general classes of mechanisms that create aggregates in protein polymerisation processes. (a) Primary nucleation pathways<sup>1,2,29</sup> result in the formation of new aggregates from interactions solely between soluble monomers. (b) Monomer-independent secondary processes,<sup>27,30,31</sup> such as fragmentation, generate new aggregates at a rate that depends only on the level of aggregates. (c) Monomer-dependent secondary pathways,<sup>9,26</sup> such as surface-catalysed nucleation, create aggregates at a rate that depends on the concentrations of both monomeric protein and existing aggregates. The rate constants are labeled  $k_n$ ,  $k_-$  and  $k_2$ , respectively, and the nucleation reaction orders with respect to the monomeric peptide are denoted  $n_c$  and  $n_2$ , as described in the text.

integrated rate law for such a system undergoing linear polymerisation and showed that it described the time course of actin polymerisation. This framework was extended in a very significant manner in the 1980s by Eaton, Ferrone, Hofrichter and coworkers who introduced the processes of heterogeneous nucleation and filament fragmentation through their pioneering studies of the kinetics of the polymerisation of hemoglobin S.<sup>7–9</sup> These secondary pathways allow new aggregates to be formed through processes that involve existing aggregates,<sup>25–28</sup> in addition to homogeneous nucleation that depends only on the level of soluble monomer (Fig. 1). In particular, filament fragmentation has emerged as a major form of secondary pathway for the proliferation of both amyloid fibrils and prion aggregates<sup>27,30,32–34</sup> *in vitro* and *in vivo*.

The nonlinear nature of the rate equations, which result from a description that includes secondary pathways, makes it problematic to analyse them. This situation implies that the integration of these equations to obtain closed form expressions describing the full time course of aggregation reactions is significantly more challenging than for simple chemical transformations or even for the nucleated polymerisation problem in the absence of secondary pathways. Progress has, however, been made through perturbative treatments<sup>9,25</sup> and recently through the derivation of self-consistent solutions,<sup>30,35–37</sup> resulting in highly accurate solutions to the rate equations now being available for the general case including both primary and secondary pathways coupled to growth processes. Here we review some of the important features of linear growth phenomena of the type encountered in amyloid assembly, using a combination of classical and modern kinetic theories,<sup>1,2,7–9,25,30,35–38</sup> which together provide the link between macroscopic measurements and the microscopic steps in the mechanism of aggregation.

## The Mechanism and Molecular Basis of Amyloid Formation

What do we mean by elucidating the mechanism of a complex conversion process, such as amyloid formation, where multiple inter-conversions are taking place simultaneously? At the most detailed level, we would like to list the processes relevant to the growth phenomenon that can occur in a given system, to define their relationships to the other processes that are accessible to generate a network of possible paths from products to reactants, and to quantify the rates at which these molecular level conversions take place. This knowledge then allows the behaviour of the system to be predicted when conditions are varied, as predictive power is a key test of any theory.

Prior to the availability of integrated rate laws for amyloid assembly, common practice has been to focus on phenomenological models and describe the reaction in terms of effective growth rates or lag phases. It is important to note, however, that these properties do not, on their own, inform on the microscopic mechanisms at play, although they are important in documenting and classifying the type of aggregation behaviour that can be observed. Rate laws are required in order to allow the connection to be established between these phenomenological parameters and the microscopic events in the system.

It is therefore instructive to consider the classes of processes that can contribute to protein aggregation phenomena. In broad terms, these processes can be divided into three categories: (i) nucleation and fragmentation processes that increase the number of aggregates, (ii) growth processes that lead to the increase in the sizes of existing aggregates and (iii) dissociation or degradation processes that lead to

the decrease in size and/or the disappearance of aggregates.

(i) *Nucleation and fragmentation processes*: These processes are responsible for increasing the number of aggregates and can broadly be grouped on the basis of their dependencies on the concentrations of free monomeric polypeptide molecules and of existing aggregates, as shown in Fig. 1. In particular, the polymerisation of a range of functional filaments, such as actin<sup>2</sup> and tubulin,<sup>39</sup> has been shown to proceed through primary nucleation, as has the aggregation of some polyglutamine species.<sup>40</sup> Furthermore, secondary pathways, which include filament fragmentation and secondary (i.e., heterogeneous) nucleation processes, such as surface-catalysed nucleation, have been shown to play a key role in the aggregation mechanism of many systems.<sup>9,26,27,30,41</sup> The relationship between bulk experimental measurements of the time course of the reaction and the microscopic nucleation steps that generate new aggregates is a major objective of mechanistic studies of amyloid formation.

(ii) *Growth processes*: Aggregates, once formed by nucleation processes, can grow by sequestering further soluble protein molecules. Interestingly, kinetic studies probing the elongation of amyloid fibrils reveal a first-order concentration dependence on both the monomer and the fibril<sup>27,42,43</sup> species, suggesting a bimolecular mechanism of growth by monomer addition to the ends of existing fibrils. In particular, this first-order concentration dependence is not consistent with growth through oligomer addition since the population of oligomers has in general a nonlinear dependence on the concentration of monomer. This example highlights the power of kinetic studies in elucidating the reaction mechanism even in the context of complex transformations. At high concentrations, the structural reorganisation of the polypeptide molecule subsequent to its attachment to the fibril end becomes rate limiting for the overall elongation process, and in this regime a transition to a zeroth-order dependence on the monomer concentration has been observed.<sup>27,42–44</sup>

(iii) *Dissociation processes*: The dissociation of molecules from aggregates is crucial in order for chemical equilibrium to be restored at the end of the aggregation reaction. This reversible and dynamical dissociation leads to the phenomenon of molecular recycling,<sup>45</sup> where the molecules in the aggregates are in constant exchange with the pool of molecules in solution and a slow turnover is observed between populations in solution and in the

aggregates. In order for aggregate growth to occur, the dissociation processes have to be significantly slower than the growth processes, and hence the dissociation phenomena are not usually of high importance in defining the kinetics of *in vitro* aggregation until very late in the reaction when the monomer pool has been exhausted.<sup>37</sup> In addition to the dissociation of monomeric peptide from aggregates, it is interesting to note that fragmentation, in addition to increasing the number of aggregates, can also play a significant role in the establishment of chemical equilibrium, unlike primary or secondary nucleation which depend on the availability of free monomer and are hence of lesser importance at very late stages in the reaction.<sup>37</sup>

## The Kinetic Profile of the Reaction Time Course

Kinetic studies provide a particularly valuable route for characterising the generation of new aggregates using bulk experimental data since this approach bypasses the difficulty in detecting low numbers of individual small species.<sup>46,47</sup> The formation of amyloid fibrils *in vitro* is commonly monitored by optical methods, including fluorometric assays relying on probes with a high affinity for the amyloid scaffold. These measurements can be designed<sup>48</sup> to report on the fraction of protein that has been sequestered into aggregates as a function of time (Fig. 2). The fundamental photophysics and binding stoichiometry that underlie these label-based approaches have, however, not been elucidated fully to date, and therefore it remains crucial to verify on a case-by-case basis the dependence of the signal on the concentration of aggregated protein molecules. This aspect is of particular importance since a nonlinear dependence will alter the shape of the reaction time course and would distort the mechanistic information that is derived from it.

The reaction time course can vary considerably in shape and symmetry for different peptides and proteins and under different reaction conditions for the same polypeptide molecule, a fact that has proved difficult to reconcile within a single model or framework. A variety of phenomenological approaches have, therefore, been put forward to describe and classify these bulk measurements. Many such approaches involve partitioning the time course into distinct phases: for example, a lag phase, a growth phase and a plateau phase. This partitioning is useful for documenting the shape of the reaction time course; a key feature of complex assembly

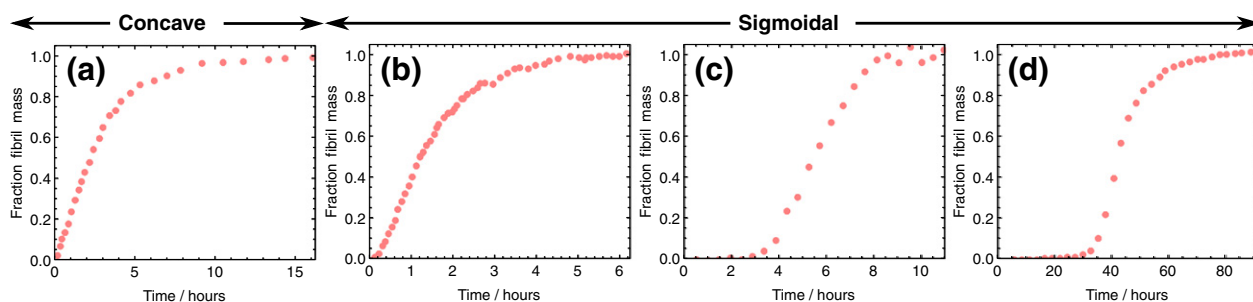


**Fig. 2.** Distinguishing contributions from growth and nucleation through the concave or convex shape of the reaction profile at early stages as described in the text. Representative examples of the broad variation in kinetic profile shapes observed for *in vitro* amyloid formation are shown. The kinetic profile is generally either concave (a) or sigmoidal (b–d); in the latter case, a variety of sigmoidal profiles, with different asymmetries, can be observed. (a) shows data for pre-seeded  $\beta_2$ -microglobulin aggregation.<sup>28</sup> The reactions in (b), (c) and (d) are from solutions initially in purely monomeric form: (b) shows data for actin polymerisation,<sup>49</sup> (c) shows data for Ure2p yeast prions<sup>50</sup> and (d) shows data for islet amyloid polypeptide aggregation.<sup>26</sup>

pathways, however, is that it is rare to find regions in time or parameter space where only a single process is active, and more commonly many forms of interconversion between the different species are operating concurrently.

An important corollary of this conclusion is that the lag phase cannot be in general defined as the time required for primary nucleation, as is sometimes assumed, even though this identification could be tempting from an intuitive point of view. Indeed, for all situations except reactions in very small volumes,<sup>46</sup> both nucleation and growth processes contribute to the length of the observed lag phase since both processes are taking place in this period.<sup>2,8,9,30,35,46</sup> Similarly, the maximal slope of the sigmoidal reaction time course, sometimes taken to correspond to the elongation rate of the aggregates present in solution, depends in general on both growth and nucleation processes.<sup>30,35</sup> More generally, it has been shown that all of the major phenomenological parameters (lag time, half-time, time to completion, maximal growth rate, etc.) depend in fact on combinations of multiple microscopic rate constants.<sup>1,2,7–9,25,30,35,36</sup> These connections between the macroscopic findings that characterise protein aggregation phenomena and their microscopic origins emerge naturally from the general theory of fibrillar growth that we discuss in this paper, which considers the possible interconversions between aggregates of different sizes and seeks to establish general rate laws for the time evolution of the system.

### Convexity in the Reaction Time Course Informs upon Nucleation Processes

Reaction time courses associated with *in vitro* aggregation and amyloid assembly exhibit a wide

range of characteristic shapes and asymmetries (Fig. 2). A very basic distinction is the concave, as in Fig. 2a, or sigmoidal, as in Fig. 2b–d, nature of the reaction time course. For reactions that are initiated entirely from monomeric peptides and in many cases for reactions that also include preformed seed material, a common characteristic is the sigmoidal, rather than concave, nature of the growth profile.

Let us first consider the reaction time course that would emerge in the case where the reaction is pre-seeded with a certain fixed number of aggregates, and there is no nucleation of new structures or fragmentation of existing aggregates. For such a system, the total number of aggregates at any time in the growth reaction is equal to the initial number of aggregates. Under these conditions, new aggregate mass is created only by incorporation of soluble monomeric peptide molecules on to the ends of existing aggregates. In such a reaction, the increase in aggregate mass, i.e. the slope of the reaction time course, is described by:

$$\text{slope} \propto [\text{monomer}] \times \overbrace{\text{no. of aggregates}}^{\text{constant}} \quad (1)$$

i.e.

$$\text{slope} \propto [\text{monomer}]$$

where the proportionality constant between the left- and right-hand sides in the first line of Eq. (1) is the rate constant for elongation. Equation (1) shows that the slope of the reaction time course is directly proportional to the concentration of free monomers, which is maximal at the beginning of the reaction and decreases monotonically. In the absence of nucleation and fragmentation, therefore, for any system with an elongation rate that has a linear (or indeed any monotonic) dependence on the monomer concentration (as required by mass action), the growth rate is maximal initially and decreases thereafter (Fig. 1a). This situation corresponds to



simple first-order kinetics characterised by an exponential approach to equilibrium.

From these very general considerations it is clear that in order to observe an overall conversion rate that increases with time in the early stages of amyloid formation, as in Fig. 1b–d, the number of aggregates in Eq. (1) must increase with time rather than remain constant<sup>†</sup>. Processes that increase the number of aggregates are classified as nucleation (or fragmentation) phenomena and include primary and secondary pathways as discussed below. In particular, for a sigmoidal rate profile to emerge, the number of aggregates must increase sufficiently quickly for the product (monomer concentration  $\times$  no. of aggregates) to increase with time even as the monomer concentration is decreasing. A concave reaction time course corresponds to the case where this product always decreases with time; in such a case, it may still be that nucleation processes are occurring, but not at a rate high enough to overcome the depletion in monomer concentration and lead to an overall increasing growth rate.

These basic considerations show that the initial phase of the time course of a sigmoidal reaction, which is defined by an increasing growth rate even as the monomer concentration is decreasing, is therefore unambiguous evidence for the presence of a nucleation or fragmentation process where new aggregates are being generated. This nucleation process may be a primary or a secondary pathway, or both, and further analysis is required to distinguish these two possibilities.

### Seeded Experiments Allow Distinction between Primary and Secondary Pathways

A sigmoidal reaction time course always indicates the generation of new aggregates during the progress of the reaction by nucleation or fragmentation. Once the role of nucleation has been identified, the next step is to characterise this process; in principle, the nucleation rate may depend on the concentration of monomeric peptide, the concentration of existing aggregates, or both (Fig.

<sup>†</sup> When the number of aggregates is not constant, an additional term is present in Eq. (1) that describes the generation (or loss) of new aggregate mass directly through nucleation (or fragmentation). In the case of protein aggregation where large aggregates form (as is the case for amyloid and many other aggregation reactions), it must be that the generation of aggregate mass through nucleation is not significant compared to that due to the growth of aggregates, and so, the additional term is small and Eq. (1) still holds.<sup>1</sup>

1). Ever since the discovery of the importance of secondary pathways in protein aggregation<sup>9,26,27,32</sup> that act in addition to the primary nucleation pathways included in the classical theory of nucleated polymerisation,<sup>1,2</sup> it has become clear that one of the most important mechanistic questions relating to the aggregation behaviour of a given molecular system is the importance of primary *versus* secondary nucleation. Indeed, it is clear that any protein that is able to form amyloid fibrils from a solution in which it was initially in purely monomeric form must be able to undergo primary nucleation (Fig. 1a) since in the absence of this process the polypeptide molecules remain in solution indefinitely. A critical question, which is less trivial to answer, is whether secondary processes (Fig. 1b and c) are also active, and to determine the relative significance of primary and secondary pathways as the reaction progresses.

One unambiguous method of determining whether or not fragmentation or secondary nucleation is active is to perform experiments within a regime where it is known that primary nucleation is only very slowly (or not at all) generating new aggregates. Thus, detection of the rapid creation of aggregates within this regime must be the result of secondary pathways. A particular strength of this strategy is that it is not necessary to have any knowledge of the detailed kinetics of the nucleation processes, and so it can be used to distinguish fragmentation or secondary nucleation from potentially very complex and poorly understood primary nucleation processes. In addition, this approach is robust to the presence of high levels of experimental noise, as it does not rely on the detailed shape of the reaction profile beyond whether it is concave or sigmoidal.

To carry out this strategy in practice, preformed seeds are used to accelerate a reaction such that it reaches completion before the equivalent reaction without preformed seeds has progressed significantly (Fig. 3). The observation of a sigmoidal profile in the presence of preformed seeds indicates the creation of many new aggregates, but the corresponding curve in the absence of preformed seeds demonstrates that primary nucleation is not creating aggregates rapidly enough during this time window to explain this effect, which by deduction must be due to a secondary pathway.

### Determination of the Reaction Order of the Nucleation Process

Crucial insights into the mechanism of a reaction can be obtained from the knowledge of the reaction order. Once the nature of the dominant nucleation process has been established as discussed in [The Mechanism and Molecular Basis of Amyloid Formation](#) and [Seeded Experiments Allow Distinction between Primary and Secondary Pathways](#), its

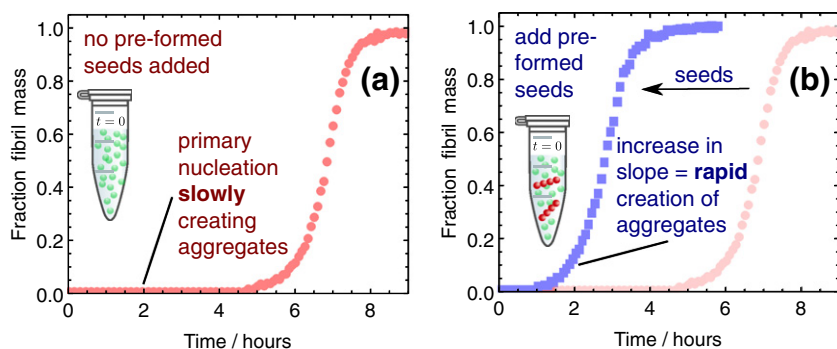


**Fig. 3.** Illustrating the problem of distinguishing secondary nucleation from primary nucleation. Secondary pathways can be identified unambiguously through the use of pre-seeded assays, as illustrated here with data for glucagon aggregation.<sup>51</sup> (a) In the absence of preformed seeds, aggregates are only generated (via primary and/or secondary pathway) at a slow rate during the first 5 h of the time

course of the reaction, as indicated by the constant (approximately zero) slope of the rate profile. (b) When preformed seeds are added at the beginning of the reaction, the kinetic profile reaches saturation before the corresponding reaction without preformed seeds has generated significant aggregate mass; in particular, the rapid increase in the slope after ca. 2 h in (b) indicates rapid creation of new aggregates. The matched profile without preformed seeds shows that primary nucleation is not rapidly creating new aggregates at this time, and by definition, the addition of seeds cannot affect primary nucleation, pinpointing the origin of the new aggregates as the effect of secondary pathways.

reaction order with respect to the monomer can be established by analysing a set of kinetic data acquired for different concentrations of the monomeric precursor peptide or protein. For instance, if aggregates are created by the dominant mechanism at a rate:

$$\text{rate of creation} \propto [\text{monomer}]^n \quad (2)$$

then  $n$  is the reaction order of the nucleation process; for primary nucleation, we write  $n_c$  and for secondary pathways,  $n_2$ . The values of  $n_c$  and  $n_2$  relate in the most simple nucleation reaction schemes to the number of monomers in the nuclei; in the more general case, however, they simply describe the leading order dependencies of the nucleation processes on the monomer concentration. Remarkably, it has been shown that the value of  $n$  can be extracted from the scaling behaviour of the phenomenological parameters (lag time, maximal growth rate, end-point, etc.) exhibited in experimental data.<sup>2,9,25,30,36</sup> One particularly convenient scaling law relates the time at which half of the monomeric protein has been sequestered into aggregates to the total initial monomer concentration as a power law:<sup>35,36</sup>

$$\text{half-time} \propto (\text{initial monomer concentration})^\gamma \quad (3)$$

where the scaling exponent  $\gamma$  is given in Table 1 and can be used to determine  $n_c$  for a system dominated by primary nucleation or  $n_2$  for a system dominated by a secondary pathway. Equation (3) becomes a linear relationship with slope equal to  $\gamma$  when plotted as a log–log plot (Fig. 4), allowing a simple extraction of the reaction order. It is interesting to note that  $\gamma = -1/2$  implies that  $n_2 = 0$ , which corresponds to a monomer-independent secondary pathway, whereas  $n_2 > 0$  corresponds to a monomer-dependent process. A similar analysis can be performed by considering the lag phase prior to the observation of aggregates by bulk methods; an advantage of considering the half-time is that it is not reliant on measurements in the lag

phase where by definition the measured signal is very weak and experimental noise can become overriding.

## Analysis of the Shape of the Reaction Time Course

It is an intriguing observation that the aggregation reactions of different peptides and proteins result in time courses with a wide range of shapes. In this section, we discuss the features that emerge in the reaction profile due to the relative influence of primary and secondary nucleation processes (Table 2), following the classic review by Ferrone.<sup>25</sup>

Typically, experimental time courses of amyloid growth are characterised by a significant influence from phenomena other than the specific process under study, including the presence of impurities and also nonlinearities in the relationship between the measured signal and the concentration of aggregates formed. Therefore, an analysis of the shape of a single curve is in general not, on its own, a definitive indicator of the molecular mechanisms at play.<sup>25</sup> In this case, a global analysis of a larger data set, acquired under conditions where parameters are varied in a systematic way, is required. This approach is discussed in [Determination of the Microscopic Rate Constants by Global Fitting](#), but it is nevertheless interesting to review here some of the links between the specific features expected in

**Table 1.** The scaling exponent  $\gamma$ , for the half-time defined in Eq. (3), is related to the reaction order of the dominant mechanism that is responsible for generating new aggregates, denoted  $n_c$  or  $n_2$

|                                   | Primary pathway  | Secondary pathway  |
|-----------------------------------|------------------|--------------------|
| Scaling exponent $\gamma \approx$ | $-\frac{n_c}{2}$ | $-\frac{1+n_2}{2}$ |

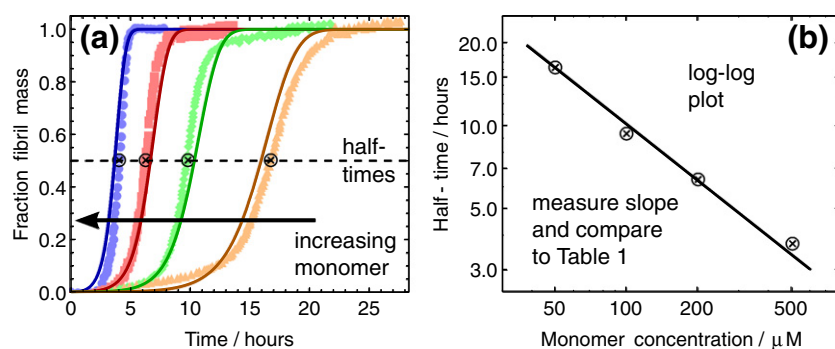


Fig. 4. Elucidation of the half-time scaling and global fitting of data, illustrated for the aggregation of the WW domain.<sup>52</sup> (a) Data for increasing initial monomer concentration. Based on the analysis of the half-times in (b), the data are fitted globally with the integrated rate law for fragmenting filaments;<sup>30,35,36</sup> the two global combined rate parameters are fixed ( $k_+, k_- = 1.5 \times 10^{-3} \text{ M}^{-2} \text{ s}^{-2}$ ,  $k_+, k_- = 2.2 \times 10^{-4} \text{ M}^{-1} \text{ s}^{-2}$ ) to provide the best fit for all four curves, as described in the main text. (b) The half-times for each initial monomer concentration are extracted from (a) and plotted against the initial monomer concentration on a log-log plot. The slope, here around  $-1/2$ , is compared with Table 2 to extract the reaction order; in the present case, the system is controlled by a secondary pathway with  $n_2 = 0$ , implying filament fragmentation as the dominant mechanism for the creation of new aggregates.

the reaction time course and the microscopic mechanisms, without making any detailed assumptions about the nucleation processes.

### Primary nucleation leads to a polynomial phase early in the reaction time course

At early stages in the reaction, the concentration of free monomer is approximately constant since it has not yet been significantly depleted by the growing aggregates. In this regime, a connection can therefore be expected between the reaction time course and the role of aggregates in the nucleation process. By contrast, at later stages, the free monomer becomes depleted as the aggregate mass approaches saturation; in this regime, a connection between the shape of the reaction profile and the nature of the growth processes is expected.

The form of the initial increase in a sigmoidal reaction time course describing protein aggregation has been studied extensively over the last five decades.<sup>1,2,7-9,25,35,53-55</sup> For many simple primary nucleation reaction schemes,<sup>6,25,56-64</sup> the early-time rise in the reaction time course is quadratic in time,  $\sim t^2$ . For more complicated primary nucleation processes involving intermediate species, sometimes known as cascade nucleation,<sup>25</sup> the early-time rise in the sigmoidal reaction time course remains polynomial, but with a cubic<sup>39</sup> or higher dependence on time,  $\sim t^m$  for a constant  $m$ .

By contrast, as noted by Eaton, Ferrone and coworkers, a reaction dominated by secondary nucleation undergoes an exponential increase in the early stages of the reaction,<sup>7,8,9</sup> as a result of the positive feedback that is a consequence of the fact that aggregates that are formed accelerate the rate of production of further aggregates.

While a polynomial increase during the early stages of aggregation precludes a dominant role for

secondary pathways, a prolonged lag followed by a rapid onset of growth in the reaction time course is indicative of the exponential behaviour characteristic of fragmentation or secondary nucleation. In the latter case, however, it is important to note that it is not always possible in practice to distinguish a high-order polynomial, for example,  $\sim t^{30}$ , which might emerge from a complex multistep primary nucleation process, from an exponential rise characteristic of secondary pathways. Such a discrimination based on the shape of a single curve remains difficult even in the absence of experimental noise. Complementary strategies, such as the procedure outlined in [Seeded Experiments Allow Distinction between](#)

**Table 2.** The early- and late-time forms of the reaction time course provide information on the dependency of the dominant nucleation or fragmentation process on the levels of free monomer and of aggregates, as discussed in the main text

|            |   | Early stage                |                                       |
|------------|---|----------------------------|---------------------------------------|
|            |   | Polynomial<br>$M \sim t^n$ | Exponential<br>$M \sim e^{kt}$        |
| Late stage | Exponential<br>$M \sim 1 - ae^{-k \cdot t}$     | Primary pathway            | Monomer-dependent secondary pathway   |
|            | Super exponential<br>$M \sim 1 - be^{-ce^{kt}}$ | N/A                        | Monomer-independent secondary pathway |

A polynomial early-time form together with an exponential late-time form is shown in Fig. 2b (primary nucleation pathway). Exponential early- and late-time forms are manifested in Fig. 2d (monomer-dependent secondary nucleation pathway). An exponential early-time form and a super exponential (Gompertz) late-time form are shown in Fig. 2c (monomer-independent secondary pathway). A polynomial early-time form and a super exponential late-time form are not commonly observed together, although mechanisms can be proposed that lead to this overall form for the reaction profile<sup>‡</sup>.



**Primary and Secondary Pathways**, make it possible, however, in all cases to distinguish unambiguously the presence of secondary pathways from a complex multistep primary nucleation pathway.

### Monomer-dependent nucleation leads to an exponential approach to saturation

While the form of the increase in the early stages of the reaction is determined primarily by whether the dominant nucleation process depends on the aggregate concentration (as in fragmentation or secondary nucleation, showing an exponential time course) or not (as in primary nucleation, showing a polynomial time course), the form of the reaction time course for later stages reveals information about the dependence of the rate of creation of aggregates on the level of free monomer.<sup>36</sup> After the rise during the early stages, there is a point of inflection in the sigmoidal reaction time course, beyond which the slope is decreasing rather than increasing; eventually, this situation leads to the profile approaching a plateau, observed once the monomer concentration has reached its equilibrium value. The form of the reaction profile that leads to the plateau differs greatly from system to system. In some cases, the early-time rise may be brief (e.g., Fig. 1b), with a slow decay towards the plateau; in other cases, the early-time rise is extended, with a sharp transition to the plateau (e.g., Fig. 1c).

At late times, as the monomer becomes heavily depleted, the shape of the reaction time course is determined primarily by the process with the weakest dependence on the monomer concentration,  $m$ . The elongation rate is linearly dependent on the monomer concentration,<sup>2,27,42,43</sup>  $\sim m$ , so unless there is a nucleation or fragmentation process with a weaker than linear dependence on the monomer concentration,  $\sim m^n$  with  $n < 1$ , the rate of generation of new aggregates will become insignificant in comparison to the rate of elongation under conditions where the monomer is depleted. Indeed, for small enough monomer concentrations,  $k_+m \gg k_N m^n$  for any elongation rate constant  $k_+$  and nucleation rate constant  $k_N$  when the reaction order  $n > 1$ . In this case, the shape of the curve will approach that of the concave reaction time course that emerges in pre-seeded growth in the absence of nucleation; that is, the decays towards equilibrium in Fig. 2b and d at late times is of the same form as that in Fig. 2a,  $\sim 1 - e^{-k_\infty t}$ .<sup>36</sup> In addition, the higher the dependence of the active nucleation processes on the monomer concentration are, the less monomer depletion is required to cause a transition to the late-time exponential saturation behaviour. If the decay is sharper than this exponential decay (e.g., Fig. 1c), it implies that a process must be active with a weaker than linear dependence on the monomer concentra-

tion,  $\sim m^n$  with  $n < 1$ ; the most common example of this behaviour is a monomer-independent process, for which  $n = 0$ , such as filament fragmentation,<sup>30,35,36,37</sup> although other processes are possible<sup>‡</sup>.

### Determination of the Microscopic Rate Constants by Global Fitting

Much of the discussion in this review article has been very general, and the mechanistic conclusions are not dependent on the specific rates of the dominant nucleation pathways. The classical framework of Oosawa and Eaton considers the most general classes of processes that generate new aggregates (Fig. 1), which have each been shown to be active in various amyloid systems, as well as the growth and shrinkage of aggregates.<sup>2,9</sup> Additional microscopic steps can, however, be added within this framework, as new experimental evidence becomes available. The benefit of a rigorous kinetic model is that the rate constants that can be extracted from the analysis of experimental data are true microscopic rate constants that are independent of the monomer concentration and so remain constant across data measured at varying concentrations of polypeptide molecules.

Recently, integrated rate laws have been derived that solve the classical framework of filamentous growth<sup>30,35,36</sup> in the presence of generalised secondary pathways; these integrated rate laws describe the growth of filaments through primary and secondary nucleation, coupled with growth through monomer addition. The closed form rate law that emerges for such a system depends in many cases primarily on only two specific combined rate parameters: the product of the elongation and the

<sup>‡</sup> Late-time super-exponential behaviour could be generated, for example, by a cascade primary nucleation scheme<sup>25,39</sup> with a monomer-independent conversion rate between intermediates that corresponds to significantly longer than the half-time of the overall aggregation reaction. In this case, beyond early times in the reaction, new growth-competent aggregates would be created at a rate independent of the monomer concentration, leading to super-exponential behaviour in the late stages of the reaction profile. In the absence of secondary pathways, this late-time form would be observed in conjunction with the classical polynomial behaviour for the early stages in the reaction that is observed for primary nucleated systems. Interestingly, on the other hand, such a mechanism if active alongside a monomer-dependent secondary nucleation process would result in that case in early-time exponential behaviour and late-time super-exponential behaviour, appearing similar to a monomer-independent secondary process. We are not aware of any system that has been shown to exhibit this behaviour at the present time.



primary nucleation rate constants, and the product of the elongation and the secondary pathway rate constants (i.e.,  $k_+k_n$  and  $k_+k_2$  where  $k_+$  is the elongation rate constant,  $k_n$  is the rate constant for the primary nucleation pathway and  $k_2$  is the rate constant for the secondary pathway, denoted instead as  $k_-$  in the case of filament fragmentation). In addition, the initial conditions of the system, including the initial concentration of free monomeric polypeptide molecules, are parameters in the final rate law. Experimental data can, therefore, be fitted globally, thereby fixing the two combined rate parameters for all curves. An example of this approach is shown in Fig. 4, where the curves are fitted with the values of  $k_+k_n$  and  $k_+k_-$  fixed globally for all four curves. The ability to capture the characteristic features of a data set with a small number of free global parameters implies that the model being used is indeed capturing the key physical characteristics of the system. It is important to note that any individual curve can be fitted by a number of sigmoidal functions, of which there are many available, and therefore, no discrimination between the mechanisms is available unless a global analysis is performed.

In order to determine the values of the individual rate constants ( $k_+$ ,  $k_n$ ,  $k_2$ ), an approach can be used where seed material is added at the beginning of the reaction, allowing the elucidation of the magnitude of the elongation rate constant,  $k_+$ , in isolation. Indeed, if sufficient seed material is added at the beginning of the reaction, then the reaction profile becomes concave, as in Fig. 1a. The initial slope of such a rate profile is equal to the product of the elongation rate constant and the number of aggregates added at the start of the reaction [Eq. (1)]; the latter is itself equal to the mass concentration of seed material added, which should be known, divided by the average number of peptides in each seed structure, which can be estimated experimentally (e.g., using atomic force microscopy<sup>30</sup>). Other experimental techniques, such as the use of a quartz crystal microbalance,<sup>43,65</sup> can alternatively be used to determine directly the elongation rate constant. Once this value is known, the rate constants for primary and secondary nucleation,  $k_n$  and  $k_2$ , can be calculated from the previously determined combined rate constants  $k_+k_n$  and  $k_+k_2$ .

## Mechanistic Implications from Kinetic Results

The type of kinetic analysis reviewed in the present work provides a window into the mechanisms of amyloid formation. A systematic study of the kinetic profiles of amyloid formation allows a characterisation of the active nucleation processes, as well as a determination of the microscopic rate

constants for the pertinent steps in the assembly pathway. In particular, it is possible to determine whether most new aggregates are being created through a process that depends only on the concentration of soluble monomer, only on the level of existing aggregates, or on both of these levels. Recent evidence suggests that small oligomeric aggregates play a key role in amyloid-related pathogenesis, and so the dependence of the rate of creation of new oligomers on the various species is of critical importance.<sup>66–68</sup>

A monomer-independent secondary mechanism,  $n_2=0$ , can be realised through filament fragmentation, which has in particular been shown to be active in the propagation of prions<sup>27</sup> and the aggregation *in vitro* of polypeptide molecules such as insulin.<sup>30</sup> A monomer-dependent secondary nucleation process,  $n_2>0$ , implies interactions between the soluble monomeric species and fibrils. Since the monomers cannot penetrate inside the fibril, this interaction must take place at the surface of the aggregates and is therefore likely to correspond to surface-catalysed nucleation, whereby new aggregates are generated from monomeric peptide molecules at the surface of existing aggregates.<sup>9</sup> Through kinetic studies, this process has been shown to be of defining importance in systems ranging from sickle-hemoglobin<sup>9</sup> to islet amyloid polypeptide.<sup>26</sup> In addition, a monomer-dependent secondary pathway may correspond in the special case of  $n_2=1$ , that is, a linear dependence on the concentration of monomer, to lateral growth and branching, factors that have been suggested to play a role, for example, in the aggregation of glucagons<sup>69</sup> and collagen.<sup>8</sup>

Importantly, secondary nucleation processes result in positive feedback, since existing aggregates play a role in accelerating the production of further aggregates. In the case of surface-catalysed nucleation, large aggregates provide surfaces at which new aggregates can be continuously generated from monomeric peptide or protein.<sup>25</sup> Moreover, frangible filaments may act as a source of small aggregates that form through breakage, even after the monomer pool has been depleted.<sup>37</sup>

It is also interesting to note that, in the case of a system that is initially in a purely monomeric form, there must be a timescale, however brief, within which primary nucleation is dominant, even if the bulk reaction kinetics are dominated by secondary nucleation. Even in a reaction where the time course is initially exponential over experimentally measurable timescales, at short enough times, the time course must always undergo a transition from an initially polynomial to an exponential profile. This fact emerges since secondary nucleation cannot become active until aggregates exist, and so there is always a phase where the rate of creation of aggregates through primary nucleation exceeds that through secondary pathways.

## Conclusions

We have discussed how a systematic analysis of bulk experimental measurements in terms of chemical kinetics provides detailed insights into the microscopic mechanisms and rate constants of protein aggregation. This knowledge is of particular interest for defining the most significant steps in the aggregation process of specific systems under a range of conditions and for understanding the origins of disease-related species. Such an understanding has the potential to shed light on the manner in which natural mechanisms provide a defence against the onset of pathogenic behaviour and on the manner in which changes such as mutation or gene duplication can give rise to disease.

## Acknowledgements

We acknowledge support from the Schiff Foundation (S.I.A.C.), the Kennedy Memorial Trust (S.I.A.C.), the Wellcome Trust (M.V., C.M.D., T.P.J.K.) and the Biotechnology and Biological Sciences Research Council (M.V., C.M.D., T.P.J.K.).

## References

- Oosawa, F. & Asakura, S. (1975). *Thermodynamics of the Polymerization of Protein*. Academic Press.
- Oosawa, F. & Kasai, M. (1962). A theory of linear and helical aggregations of macromolecules. *J. Mol. Biol.* **4**, 10–21.
- Tobacman, L. S. & Korn, E. D. (1983). The kinetics of actin nucleation and polymerization. *J. Biol. Chem.* **258**, 3207–3214.
- Frieden, C. & Goddette, D. W. (1983). Polymerization of actin and actin-like systems: evaluation of the time course of polymerization in relation to the mechanism. *Biochemistry*, **22**, 5836–5843.
- Wegner, A. & Engel, J. (1975). Kinetics of the cooperative association of actin to actin filaments. *Biophys. Chem.* **3**, 215–225.
- Hofrichter, J., Ross, P. D. & Eaton, W. A. (1974). Kinetics and mechanism of deoxyhemoglobin s gelation: a new approach to understanding sickle cell disease. *Proc. Natl Acad. Sci. USA*, **71**, 4864–4868.
- Ferrone, F. A., Hofrichter, J., Sunshine, H. R. & Eaton, W. A. (1980). Kinetic studies on photolysis-induced gelation of sickle cell hemoglobin suggest a new mechanism. *Biophys. J.* **32**, 361–380. [http://dx.doi.org/10.1016/S0006-3495\(80\)84962-9](http://dx.doi.org/10.1016/S0006-3495(80)84962-9).
- Bishop, M. F. & Ferrone, F. A. (1984). Kinetics of nucleation-controlled polymerization. A perturbation treatment for use with a secondary pathway. *Biophys. J.* **46**, 631–644. [http://dx.doi.org/10.1016/S0006-3495\(84\)84062-X](http://dx.doi.org/10.1016/S0006-3495(84)84062-X).
- Ferrone, F. A., Hofrichter, J. & Eaton, W. A. (1985). Kinetics of sickle hemoglobin polymerization. ii. a double nucleation mechanism. *J. Mol. Biol.* **183**, 611–631.
- Dobson, C. M. (1999). Protein misfolding, evolution and disease. *Trends Biochem. Sci.* **24**, 329–332.
- Chiti, F. & Dobson, C. M. (2006). Protein misfolding, functional amyloid, and human disease. *Annu. Rev. Biochem.* **75**, 333–366. <http://dx.doi.org/10.1146/annurev.biochem.75.101304.123901>.
- Dobson, C. M. (2003). Protein folding and misfolding. *Nature*, **426**, 884–890. <http://dx.doi.org/10.1038/nature02261>.
- Cohen, F. E. & Kelly, J. W. (2003). Therapeutic approaches to protein-misfolding diseases. *Nature*, **426**, 905–909. <http://dx.doi.org/10.1038/nature02265>.
- Selkoe, D. J. (2003). Folding proteins in fatal ways. *Nature*, **426**, 900–904. <http://dx.doi.org/10.1038/nature02264>.
- Lansbury, P. T. & Lashuel, H. A. (2006). A century-old debate on protein aggregation and neurodegeneration enters the clinic. *Nature*, **443**, 774–779. <http://dx.doi.org/10.1038/nature05290>.
- Pepys, M. B. (2001). Pathogenesis, diagnosis and treatment of systemic amyloidosis. *Phil. Trans. R. Soc. London B*, **356**, 203–210; discussion 210–211.
- Hardy, J. & Selkoe, D. J. (2002). The amyloid hypothesis of Alzheimer's disease: progress and problems on the road to therapeutics. *Science*, **297**, 353–356. <http://dx.doi.org/10.1126/science.1072994>.
- Sacchettini, J. C. & Kelly, J. W. (2002). Therapeutic strategies for human amyloid diseases. *Nat. Rev., Drug Discovery*, **1**, 267–275. <http://dx.doi.org/10.1038/nrd769>.
- Prusiner, S. B. (1991). Molecular biology of prion diseases. *Science*, **252**, 1515–1522.
- Come, J. H., Fraser, P. E. & Lansbury, P. T. (1993). A kinetic model for amyloid formation in the prion diseases: importance of seeding. *Proc. Natl Acad. Sci. USA*, **90**, 5959–5963.
- Aguzzi, A. & Haass, C. (2003). Games played by rogue proteins in prion disorders and Alzheimer's disease. *Science*, **302**, 814–818. <http://dx.doi.org/10.1126/science.1087348>.
- Falsig, J., Nilsson, K. P., Knowles, T. P. J. & Aguzzi, A. (2008). Chemical and biophysical insights into the propagation of prion strains. *HFSP J.* **2**, 332–341. <http://dx.doi.org/10.2976/1.2990786>.
- Aguzzi, A. & O'Connor, T. (2010). Protein aggregation diseases: pathogenicity and therapeutic perspectives. *Nat. Rev., Drug Discovery*, **9**, 237–248. <http://dx.doi.org/10.1038/nrd3050>.
- Oosawa, F., Asakura, S., Hotta, K., Imai, N. & Ooi, T. (1959). G-F transformation of actin as a fibrous condensation. *J. Poly. Sci.* **37**, 323.
- Ferrone, F. (1999). Analysis of protein aggregation kinetics. *Methods Enzymol.* **309**, 256–274.
- Ruschak, A. M. & Miranker, A. D. (2007). Fiber-dependent amyloid formation as catalysis of an existing reaction pathway. *Proc. Natl Acad. Sci. USA*, **104**, 12341–12346. <http://dx.doi.org/10.1073/pnas.0703306104>.
- Collins, S. R., Dougllass, A., Vale, R. D. & Weissman, J. S. (2004). Mechanism of prion propagation: amyloid growth occurs by monomer addition. *PLoS Biol.* **2**,

- e321. <http://dx.doi.org/10.1371/journal.pbio.0020321>.
28. Xue, W. F., Homans, S. W. & Radford, S. E. (2008). Systematic analysis of nucleation-dependent polymerization reveals new insights into the mechanism of amyloid self-assembly. *Proc. Natl Acad. Sci. USA*, **105**, 8926–8931. <http://dx.doi.org/10.1073/pnas.0711664105>.
  29. Serio, T. R., Cashikar, A. G., Kowal, A. S., Sawicki, G. J., Moslehi, J. J., Serpell, L. *et al.* (2000). Nucleated conformational conversion and the replication of conformational information by a prion determinant. *Science*, **289**, 1317–1321.
  30. Knowles, T. P. J., Waudby, C. A., Devlin, G. L., Cohen, S. I. A., Aguzzi, A., Vendruscolo, M. *et al.* (2009). An analytical solution to the kinetics of breakable filament assembly. *Science*, **326**, 1533–1537. <http://dx.doi.org/10.1126/science.1178250>.
  31. Wegner, A. (1982). Kinetic analysis of actin assembly suggests that tropomyosin inhibits spontaneous fragmentation of actin filaments. *J. Mol. Biol.* **161**, 217–227.
  32. Tanaka, M., Collins, S. R., Toyama, B. H. & Weissman, J. S. (2006). The physical basis of how prion conformations determine strain phenotypes. *Nature*, **442**, 585–589. <http://dx.doi.org/10.1038/nature04922>.
  33. Toyama, B. H., Kelly, M. J. S., Gross, J. D. & Weissman, J. S. (2007). The structural basis of yeast prion strain variants. *Nature*, **449**, 233–237. <http://dx.doi.org/10.1038/nature06108>.
  34. Aguzzi, A. (2004). Understanding the diversity of prions. *Nat. Cell. Biol.* **6**, 290–292. <http://dx.doi.org/10.1038/ncb0404-290>.
  35. Cohen, S. I. A., Vendruscolo, M., Welland, M. E., Dobson, C. M., Terentjev, E. M. & Knowles, T. P. J. (2011). Nucleated polymerization with secondary pathways. I. Time evolution of the principal moments. *J. Chem. Phys.* **135**, 065105. <http://dx.doi.org/10.1063/1.3608916>.
  36. Cohen, S. I. A., Vendruscolo, M., Dobson, C. M. & Knowles, T. P. J. (2011). Nucleated polymerization with secondary pathways. II. Determination of self-consistent solutions to growth processes described by non-linear master equations. *J. Chem. Phys.* **135**, 065106. <http://dx.doi.org/10.1063/1.3608917>.
  37. Cohen, S. I. A., Vendruscolo, M., Dobson, C. M. & Knowles, T. P. J. (2011). Nucleated polymerization with secondary pathways. III. Equilibrium behavior and oligomer populations. *J. Chem. Phys.* **135**, 065107. <http://dx.doi.org/10.1063/1.3608918>.
  38. Cohen, S. I. A., Vendruscolo, M., Dobson, C. M. & Knowles, T. P. J. (2011). Nucleated polymerisation in the presence of pre-formed seed filaments. *Int. J. Mol. Sci.* **12**, 5844–5852. <http://dx.doi.org/10.3390/ijms12095844>.
  39. Flyvbjerg, H., Jobs, E. & Leibler, S. (1996). Kinetics of self-assembling microtubules: an “inverse problem” in biochemistry. *Proc. Natl Acad. Sci. USA*, **93**, 5975–5979.
  40. Kar, K., Jayaraman, M., Sahoo, B., Kodali, R. & Wetzel, R. (2011). Critical nucleus size for disease-related polyglutamine aggregation is repeat-length dependent. *Nat. Struct. Mol. Biol.* **18**, 328–336. <http://dx.doi.org/10.1038/nsmb.1992>.
  41. Wegner, A. (1982). Spontaneous fragmentation of actin filaments in physiological conditions. *Nature*, **296**, 266–267.
  42. Knowles, T. P., Fitzpatrick, A. W., Meehan, S., Mott, H. R., Vendruscolo, M., Dobson, C. M. & Welland, M. E. (2007). Role of intermolecular forces in defining material properties of protein nanofibrils. *Science*, **318**, 1900–1903. <http://dx.doi.org/10.1126/science.1150057>.
  43. Buell, A. K., Blundell, J. R., Dobson, C. M., Welland, M. E., Terentjev, E. M. & Knowles, T. P. J. (2010). Frequency factors in a landscape model of filamentous protein aggregation. *Phys. Rev. Lett.* **104**, 228101.
  44. Scheibel, T., Bloom, J. & Lindquist, S. L. (2004). The elongation of yeast prion fibers involves separable steps of association and conversion. *Proc. Natl Acad. Sci. USA*, **101**, 2287–2292.
  45. Carulla, N., Caddy, G. L., Hall, D. R., us Zurdo, J., Gairi, M., Feliz, M. *et al.* (2005). Molecular recycling within amyloid fibrils. *Nature*, **436**, 554–558. <http://dx.doi.org/10.1038/nature03986>.
  46. Knowles, T. P. J., White, D. A., Abate, A. R., Agresti, J. J., Cohen, S. I. A., Sperling, R. A. *et al.* (2011). Observation of spatial propagation of amyloid assembly from single nuclei. *Proc. Natl Acad. Sci. USA*, **108**, 14746–14751. <http://dx.doi.org/10.1073/pnas.1105555108>.
  47. Orte, A., Birkett, N. R., Clarke, R. W., Devlin, G. L., Dobson, C. M. & Klenerman, D. (2008). Direct characterization of amyloidogenic oligomers by single-molecule fluorescence. *Proc. Natl Acad. Sci. USA*, **105**, 14424–14429. <http://dx.doi.org/10.1073/pnas.0803086105>.
  48. Hellstrand, E., Boland, B., Walsh, D. M. & Linse, S. (2010). Amyloid  $\beta$ -protein aggregation produces highly reproducible kinetic data and occurs by a two-phase process. *ACS Chem. Neurosci.* **1**, 13–18.
  49. Wegner, A. & Savko, P. (1982). Fragmentation of actin filaments. *Biochemistry*, **21**, 1909–1913.
  50. Zhu, L., Zhang, X. J., Wang, L. Y., Zhou, J. M. & Perrett, S. (2003). Relationship between stability of folding intermediates and amyloid formation for the yeast prion ure2p: a quantitative analysis of the effects of pH and buffer system. *J. Mol. Biol.* **328**, 235–254.
  51. Pedersen, J. S. & Otzen, D. E. (2008). Amyloid-a state in many guises: survival of the fittest fibril fold. *Protein Sci.* **17**, 2–10. <http://dx.doi.org/10.1110/ps.073127808>.
  52. Ferguson, N., Berriman, J., Petrovich, M., Sharpe, T. D., Finch, J. T. & Fersht, A. R. (2003). Rapid amyloid fiber formation from the fast-folding ww domain fbp28. *Proc. Natl Acad. Sci. USA*, **100**, 9814–9819. <http://dx.doi.org/10.1073/pnas.1333907100>.
  53. Kunes, K. C., Cox, D. L. & Singh, R. R. P. (2005). One-dimensional model of yeast prion aggregation. *Phys. Rev. E. Stat. Nonlin. Soft Matter Phys.* **72**, 051915.
  54. Masel, J., Jansen, V. A. & Nowak, M. A. (1999). Quantifying the kinetic parameters of prion replication. *Biophys. Chem.* **77**, 139–152.
  55. Poeschel, T., Brilliantov, N. V. & Froemmel, C. (2003). Kinetics of prion growth. *Biophys. J.* **85**, 3460–3474. [http://dx.doi.org/10.1016/S0006-3495\(03\)74767-5](http://dx.doi.org/10.1016/S0006-3495(03)74767-5).

56. Firestone, M. P., de Levie, R. & Rangarajan, S. K. (1983). On one-dimensional nucleation and growth of "living polymers". I. Homogeneous nucleation. *J. Theor. Biol.* **104**, 553–570.
57. Goldstein, R. F. & Stryer, L. (1986). Cooperative polymerization reactions. Analytical approximations, numerical examples, and experimental strategy. *Biophys. J.* **50**, 583–599. [http://dx.doi.org/10.1016/S0006-3495\(86\)83498-1](http://dx.doi.org/10.1016/S0006-3495(86)83498-1).
58. Ataka, M. & Ogawa, T. (1993). Nucleation and growth of oxide precipitates in cz-si wafers. *J. Mater. Res.* **11**, 2889–2992.
59. Bessho, Y., Ataka, M., Asai, M. & Katsura, T. (1994). Analysis of the crystallization kinetics of lysozyme using a model with polynuclear growth mechanism. *Biophys. J.* **66**, 310–313.
60. Lomakin, A., Teplow, D. B., Kirschner, D. A. & Benedek, G. B. (1997). Kinetic theory of fibrillogenesis of amyloid beta-protein. *Proc. Natl Acad. Sci. USA*, **94**, 7942–7947.
61. Murphy, R. M. & Pallitto, M. M. (2000). Probing the kinetics of beta-amyloid self-association. *J. Struct. Biol.* **130**, 109–122. <http://dx.doi.org/10.1006/jsbi.2000.4253>.
62. Chen, S., Ferrone, F. A. & Wetzel, R. (2002). Huntington's disease age-of-onset linked to polyglutamine aggregation nucleation. *Proc. Natl Acad. Sci. USA*, **99**, 11884–11889. <http://dx.doi.org/10.1073/pnas.182276099>.
63. Wetzel, R. (2006). Kinetics and thermodynamics of amyloid fibril assembly. *Acc. Chem. Res.* **39**, 671–679. <http://dx.doi.org/10.1021/ar050069h>.
64. Andrews, J. M. & Roberts, C. J. (2007). A Lumry–Eyring nucleated polymerization model of protein aggregation kinetics: 1. Aggregation with pre-equilibrated unfolding. *J. Phys. Chem. B*, **111**, 7897–7913. <http://dx.doi.org/10.1021/jp070212j>.
65. Knowles, T. P. J., Shu, W., Devlin, G. L., Meehan, S., Auer, S., Dobson, C. M. & Welland, M. E. (2007). Kinetics and thermodynamics of amyloid formation from direct measurements of fluctuations in fibril mass. *Proc. Natl Acad. Sci. USA*, **104**, 10016–10021. <http://dx.doi.org/10.1073/pnas.0610659104>.
66. Bucciantini, M., Giannoni, E., Chiti, F., Baroni, F., Formigli, L., Zurdo, J. *et al.* (2002). Inherent toxicity of aggregates implies a common mechanism for protein misfolding diseases. *Nature*, **416**, 507–511. <http://dx.doi.org/10.1038/416507a>.
67. Walsh, D. M., Klyubin, I., Fadeeva, J. V., Cullen, W. K., Anwyl, R., Wolfe, M. S. *et al.* (2002). Naturally secreted oligomers of amyloid beta protein potently inhibit hippocampal long-term potentiation *in vivo*. *Nature*, **416**, 535–539. <http://dx.doi.org/10.1038/416535a>.
68. Haass, C. & Selkoe, D. J. (2007). Soluble protein oligomers in neurodegeneration: lessons from the Alzheimer's amyloid beta-peptide. *Nat. Rev., Mol. Cell Biol.* **8**, 101–112. <http://dx.doi.org/10.1038/nrm2101>.
69. Andersen, C. B., Yagi, H., Manno, M., Martorana, V., Ban, T., Christiansen, G. *et al.* (2009). Branching in amyloid fibril growth. *Biophys. J.* **96**, 1529–1536. <http://dx.doi.org/10.1016/j.bpj.2008.11.024>.